Septic shock as a trigger of arterial stress-induced premature senescence: A new pathway involved in the post sepsis long-term cardiovascular complications

Hamid Merdji, Mohamad Kassem, Louise Chomel, Raphaël Clere-Jehl, Julie Helms, Kei Kurihara, Ahmed Bey Chaker, Cyril Auger, Valérie Schini-Kerth, Florence Toti, et al.

Septic shock as a trigger of arterial Stress-Induced Premature Senescence: A new pathway involved in the post sepsis long-term cardiovascular complications.

Running title: Septic shock as a trigger of arterial Stress-Induced Premature Senescence.

Hamid MERDJI[1,2], M.D., MSc., Mohamad KASSEM[1], Ph.D., Louise CHOMEL[1], MSc., Raphaël CLERE-JEHL[2], M.D., Ph.D., Julie HELMS[1,2], M.D., Ph.D., Kei KURIHARA[1,3], M.D., Ph.D., Ahmed Bey CHAKER[1], Ph.D., Cyril AUGER[1], Ph.D., Valérie SCHINI-KERTH[1], Ph.D., Florence TOTI[1], Ph.D., Ferhat MEZIANI[1,2,] M.D., Ph.D.

[1]INSERM (French National Institute of Health and Medical Research), UMR 1260, Regenerative Nanomedicine (RNM), CRBS (Centre de Recherche en Biomédecine de Strasbourg), FMTS (Fédération de Médecine Translationnelle de Strasbourg), University of Strasbourg, Strasbourg, France.

[2]Department of Intensive Care (Service de Médecine Intensive - Réanimation), Nouvel Hôpital Civil, Hôpital Universitaire de Strasbourg, Strasbourg, France.

[3]Aichi Medical University, Department of Transplantation and Regenerative Medicine, Fujita Health University, School of Medicine, Aichi, Japan.

Correspondence to:

Ferhat Meziani (MD, PhD)

Service de Médecine Intensive- Réanimation – Nouvel Hôpital Civil

1, place de l'Hôpital

F-67091 STRASBOURG cedex (France)

Phone: +33 (0) 369 550 434; Fax: +33 (0) 369 551 859

E-mail: ferhat.meziani@chru-strasbourg.fr

Nonstandard abbreviations:

SIRS: systemic inflammatory response syndrome

ICU: intensive care unit

EC: endothelial cell

MACEs: major adverse cardiac events

SIPS: stress-Induced Premature Senescence

TF: transcription factor

SASP: senescence-associated secretory phenotype

CLP: cecal ligation and puncture

PE: phenylephrine

Ach: acetylcholine

PBS: phosphate buffer saline

ROS: reactive oxygen species

NO: nitric oxide

WB: western blot

Acknowledgements:
This project received financial support from the « Association d'Aide aux Insuffisants Respiratoires d'Alsace-Lorraine (ADIRAL, Strasbourg, France) ».

Conflict of Interest statement:
No conflict of interest regarding the present manuscript has to be disclosed.

Authors' contribution:

- HM, FT and FM participated in designing the research
- HM, MK, JH, VSK, FT and FM participated in the writing and editing of the manuscript.
- HM, MK and KK performed the surgery on rat and the measurement of intra-femoral blood pressure.
- HM, MK, LC and KK performed the analyses on rat organs.
- HM, MK and KK performed the vascular reactivity.

Word count:

- Abstract: 243
- Article: 3739

At a Glance: This work provides new insights into the role of septic shock leading to stress-induced premature senescence on vascular tissue. This senescent phenotype causes endothelial and vascular dysfunction involved in atherogenesis and may partly explain the increased risk of major adverse cardiovascular events in sepsis survivors.

Abstract

Background: Major adverse cardiovascular events among sepsis survivors is an emerging health issue. Because endothelial senescence leads to vascular dysfunction and atherothrombosis, sepsis could be associated to vascular stress-induced premature senescence and thus with long-term cardiovascular events.

Materials & Methods: Adult Wistar male rats were submitted to cecal ligation and puncture, or a SHAM operation. Markers of inflammation, oxidative stress and endothelial senescence were assessed at 3, 7 and 90 days (D), and vascular reactivity was assessed in conductance and resistance vessels at D90. Expression of proteins involved in senescence and inflammation was assessed by Western blot analysis and confocal microscopy, oxidative stress by dihydroethidium probing.

Results: Pro-inflammatory endothelial ICAM-1 and VCAM-1 were up-regulated by three-fold in CLP *vs*. SHAM at D7 and remained elevated at D90. Oxidative stress followed a similar pattern but was detected in the whole vascular wall. Sepsis accelerated premature senescence in aorta vascular tissue as shown by the significant up-regulation of p53 and down-stream p21 and p16 senescent markers at D7, values peaking at D90 whereas the absence of significant variation in activated caspase-3 confirmed p53 as a prime inducer of senescence. In addition, p53 was mainly expressed in the endothelium. Sepsis-induced long-term vascular dysfunction was confirmed in aorta and main mesenteric artery, with a major alteration of the endothelial-dependent nitric oxide pathway.

Conclusions: Septic shock-induced long-term vascular dysfunction is associated with endothelial and vascular senescence. Our model could prove useful for investigating senolytic therapies aiming at reducing long-term cardiovascular consequences of septic shock.

Abstract total words: 243

Keywords: septic shock ; sepsis ; Stress-Induced Premature Senescence ; atherosclerosis.

Introduction

Sepstic shock is a life-threatening multiple organ dysfunction caused by a dysregulated host response to infection characterized by a systemic inflammatory response syndrome (SIRS), altering cardiovascular function (1) and is recognized as global health priorities by the World Health Organization (2). Although a precise estimate of the global epidemiological burden of sepsis is difficult to ascertain, sepsis was recently reported to affect worldwide 49 million people and cause 11 million deaths every year (3). In intensive care unit (ICU), sepsis is also the leading cause of mortality (4). However, long-term survival has improved, with approximately 14 million sepsis survivors each year (5) but generating a significant healthcare burden with adverse outcomes (6).

Septic shock is characterized by an endothelial cell (EC) dysfunction, affecting vascular tone and barrier's role (7), favoring systemic inflammation and coagulation activation (8) and multiple organ dysfunction. Vascular endothelium is critically involved in vascular homeostasis, including angiogenesis, blood pressure regulation, coagulation (9). Sepsis has been associated with acute and/or higher rates of cardiovascular complications linked to endothelial dysfunction, including atherothrombosis, ischemic stroke, hypertension and thrombotic events (10). The incidence of long-term cardiovascular diseases in post sepsis survivors is an emerging health issue, as indicated by recent propensity matched studies underlying an increased risk of major adverse cardiac events (MACEs) such as myocardial infarction and stroke (11). Indeed, an increased risk of mild- to long-term mortality among sepsis survivors is possibly related to an elevated rate of post-sepsis cardiovascular events as atherosclerosis (12, 13) with yet non elucidated mechanisms.

During ageing, replicative senescence occurs as a result of telomere shortening. However, senescence can also be induced in young cells exposed to exogenous stressors, phenomenon

identified as Stress-Induced Premature Senescence (SIPS) (14). In senescent cells, the transcription factor (TF) p53 is an upstream initiator (15), whereas downstream other TF as p21 and p16 inhibit the progression of the cell cycle (16). Thus, endothelial cell senescence is characterized by an irreversible cell cycle arrest and a characteristic secretion profile termed senescence-associated secretory phenotype (SASP), including growth factors, proteases, and cytokines acting as potent autocrine and paracrine effectors affecting neighbor cells (17, 18). Senescent ECs lining the vulnerable atherosclerotic plaques have been observed in human coronary arteries and aortic arches of elderly patients (19). However, to date and to the best of our knowledge, the premature or accelerated endothelial senescence are not assessed *in vivo* during septic shock.

We therefore hypothesized that septic shock syndrome may favor premature and sustained EC senescence, which in turn promotes long-term atherothrombosis. For this purpose, we established an original three months sepsis rat model to investigate vascular markers of inflammation and senescence as well as endothelial dysfunction.

Material and Methods

Study overview

We assessed long-term effects of sepsis on clinical parameters, systemic inflammation and atherothrombosis in young male Wistar rats without preexisting cardiovascular disease. Rats were submitted to cecal ligation and puncture (CLP), the "gold standard" model of sepsis in animals (20). Rats were randomly assigned to the CLP or SHAM subset and kept in the animal facility up to 3 months. Rats were sacrificed at selected time points (3, 7, 90 days) to assess lactate plasma concentration, glycemia, blood pressure, body weight, the degree of endothelial senescence, the aorta vascular tone and vascular markers of oxidative stress (Figure 1).

Ethics statement

Male Wistar rats (Janvier-Labs, Le Genest-St-Isle, France) were housed in a temperature controlled (22 °C) room and maintained on a standard 12-h light/dark cycle (lights on at 07:00 am), with free access to food and water. All aspects of this study complied with the Guide for the Care and Use of Laboratory Animals published by the National Institutes of Health (NIH Publication 85-23 (revised 1996)) and were approved by the French Ministry of Higher Education and Research and by a local Ethic Committee (Comite d'éthique en Matière d'expérimentation animale de Strasbourg, authorization number 15498). All animal experiments were done in a registered animal yard within Faculty of Pharmacy (Authorization number E 67-218-26).

Sepsis induction

Sepsis was induced by cecal ligation and puncture (CLP), a polymicrobial model of sepsis, previously described by Rittirsch et al (21). Rats (mean weight 332±30 g) were randomly

assigned to either a SHAM group or CLP group and operated as described below. During surgical procedures, rats were anesthetized with isoflurane 1–2% (Piramal Critical Care, Pennsylvania, USA) and analgesia was performed with subcutaneous buprenorphine 0.01 mg/kg of body weight (CEVA, Libourne, Fance). A subcutaneous injection of 2 mg/kg lidocaine 1% (MSD Santé Animale, New-Jersey, USA) was performed before skin incision. Under aseptic conditions, a 1.5 cm midline laparotomy was performed to allow exposure, ligation and puncture of the caecum with a 21-gauge needle. A small amount of feces was extruded, the caecum returned into the peritoneal cavity and the incision was closed using two layers of sutures. SHAM rats underwent a midline laparotomy and cecal exposure without further manipulation. All rats received a subcutaneous injection of 0.9% NaCl (5-10 ml/kg of body weight) for fluid loss immediately after the surgery. In addition, a subcutaneous injection of buprenorphine 0.01 mg/kg was done each 6 hours during 2 days. Rats had free access to standard chow and water after induction of sepsis. Three days (D3), seven days (D7) or three months (D90) after surgery, rats were sacrificed after being anesthetized with isoflurane, and whole blood collected through cardiac puncture. All rats that reached D90 were weighted (mean weight 497±23 g).

Characterization of the sepsis degree of severity

Blood lactate levels were measured as a surrogate marker of severity 1 h and 24 h after the experimental procedure (H1, H24). Blood pressure was measured 24 hours after the end of the procedure using a femoral intra-arterial line performed under anesthesia by isoflurane.

Isolation of rat aortic tissue

Aortas (3–5 cm) were harvested at day 90 (D90). Briefly, rats were anaesthetized with isoflurane. A median sternotomy was performed, and aorta were carefully excised and cut

into 0.5 cm segments for histological and biochemical analysis. Segments from the aortic cross, the thoracic and abdominal aorta were either included into OCT (frozen section compound) or directly flash frozen in liquid nitrogen and stored at -80 °C for later use.

Assessment of inflammation and senescence markers by Western blot

Proteins were extracted from the aortic tissue after grinding using liquid nitrogen by RIPA lysis buffer (20 mMTris/HCl, 150 mM NaCl, 1 mM Na3VO4, 10 mM sodium pyrophosphate, 0.01 mM okadaic acid, 20 mM, a tablet of protease inhibitor (Roche, Basel, Switzerland), and 1% Triton X-100 (Euromedex, Souffelweyershem, France). Proteins (20 μg) were separated by 10% or 12% SDS-PAGE at 100 V for 2 hours and further electrophoretically transferred onto polyvinylidene difluoride (PVDF) membrane (GE Healthcare, VWR, Fontenay-sous-Bois, France) at 100 V for 2 hours. Membrane non- specific binding sites were blocked in Tris-buffered saline (TBS) solution containing 5% BSA (Bovine Serum Albumin) and 0.1% Tween-20 (Euromedex) for 1 h at room temperature. Proteins of interest were probed with specific primary antibodies in blocking solution, rabbit monoclonal anti-VCAM-1 (ab215380, 1:1000, Abcam, UK), mouse monoclonal anti-ICAM-1 (ab171123, 1:1000, Abcam), rabbit polyclonal anti-COX-2 (ab15191, 1:1000, Abcam), rabbit polyclonal anti-Cleaved Caspase 3 (9661L, 1/1000, Cell signaling, USA), mouse monoclonal anti-p21 (sc-817, 1:1000; Santa Cruz Biotechnology, USA) and rabbit polyclonal anti-p53 (sc-6243, 1:1000; Santa Cruz Biotechnology), rabbit polyclonal anti-p16 (250804, 1:500, Abbiotec, USA) at 4 °C overnight. Membranes were washed three times with TBS-T (TBS-Tween, Euromedex) and incubated with peroxidase-labelled secondary antibodies; anti-rabbit (7074s, 3:10000, Cell signaling technology, USA) or anti-mouse (7076s, 1:10000, Cell signaling technology, USA) for 60 min, at room temperature. Immunostaining was revealed by chemiluminescence solution (ECL, Bio-Rad laboratories, USA). The chemiluminescence signal was recorded with ImageQuant LAS

4000 system (GE Healthcare Europe GmbH, Velizy-Villacoublay, France) and analyzed using ImageQuant TL software (version 8.1, GE Healthcare). Quantitative normalization with respect to β-tubulin as the housekeeping protein was performed for each protein of interest using a specific antibody (mouse monoclonal anti-beta-tubulin I T7816, Sigma-Aldrich, Missouri, USA).

Vascular reactivity

ex vivo vascular reactivity of aorta and main mesenteric artery rings was assessed as previously described (22). Briefly, the aorta or the main mesenteric artery were cleaned of connective tissue, cut into rings (2–3 mm in length) and suspended in organ baths containing oxygenated (95% O_2, 5% CO_2) Krebs bicarbonate solution (NaCl 119 mM, KCl 4.7 mM, KH2PO4 1.18 mM, MgSO4 1.18 mM, CaCl2 1.25 mM, NaHCO3 25 mM, D-glucose 11 mM, pH 7.4, at 37 °C) for the determination of changes in isometric tension. After equilibration and functional tests, rings were pre-contracted with phenylephrine (PE, 1 μM) before construction of concentration-relaxation curves to acetylcholine (ACh). In some experiments, rings were exposed to an inhibitor for 30 minutes before contraction with PE. Relaxations were expressed as percentage of the contraction induced by PE (23).

Immunofluorescence staining and confocal microscopy

Freshly dissected aorta abdominal segments were frozen with frozen section compound, cut to 14 μm section and fixed in paraformaldehyde 4% (or with Acetone: Alcohol, 50:50 mixture for anti-p53 antibody) during 30 minutes at room temperature before three washes in Phosphate buffer saline (PBS). Blocking of nonspecific binding sites was done in PBS containing 1% PFA and 0.1% Triton for 30 minutes before overnight incubation at 4 °C with either a mouse monoclonal antibody to p53 (sc-6243, 1:50; Santa Cruz Biotechnology, Germany), eNOS

(610297, 1:100; BD Bioscience, USA), iNOS (610329, 1:200; BD Bioscience, USA) or a polyclonal rabbit antibody to MMP-9, (ab38898, 1:200; Abcam, UK). After three washes, tissue sections were incubated in the dark for 1 h at room temperature with the respective secondary antibodies: Alexa fluor-633-labeled anti-mouse IgG (A21052, 1:400, Life Technologies, USA) or Alexa fluor-633-labeled anti-rabbit IgG (A21071, 1:400, Life Technologies, USA). After three washes, slides were counterstained with DAPI before being mounted under coverslip using fluorescence mounting medium (DAKO, USA), dried in the dark and analyzed.

Determination of the vascular level of reactive oxygen species

The level of oxidative stress in tissues was determined using Dihyroethidium (DHE), a redox-sensitive fluorescent probe. After incubation of the tissues with a pharmacological inhibitor for 30 minutes, reactive oxygen species (ROS) sources were identified using 2.5 µM DHE, a redox-sensitive fluorescent probe incubated for 30 min, at 37 ºC in a light protected humidified chamber. The nuclei were counterstained by DAPI labelling. After washings three time with PBS, slides were mounted under coverslip using fluorescence mounting medium (DAKO, USA), dried in dark and analyzed by confocal microscopy (Leica SP2 UV DM IRBE; Leica, Heidelberg, Germany). Fluorescence signal were quantified by Image J software after elimination of the autofluorescence signal.

Statistical analysis

Data, expressed as mean ± standard deviation (S.D.), were analyzed using GraphPad Prism8® (GraphPad Software, Inc., CA, US). “n” represents the number of animals. Mean values were compared using unpaired Student’s t-test for the comparisons of two groups for quantitative confocal microscopy results and western blot analysis. Statistical variance between different groups was determined by applying Two-way analysis of variance (ANOVA) test for vascular

reactivity studies. Survival curves were analyzed by the log-rank (Mantel-Cox) and Gehan-Breslow-Wilcoxon tests. A $p\ value < 0.05$ was considered statistically significant. All measurements were from at least three separate individuals.

Results

Septic shock induced arterial inflammation: A long-lasting effect

Twenty-four hours after CLP, a significant drop in the mean arterial pressure (MAP) was observed (CLP: 77.3±6.8 *vs.* SHAM: 99.9±2.3 mmHg, $p < 0.01$) Blood lactate concentration was accordingly significantly higher in CLP compared to SHAM (3.2±0.1 *vs.* 1.8±0.06 mM; $p < 0.01$) indicating tissue hypoperfusion and cellular hypoxia (24). Mortality only occurred in the CLP group and only during the first few days after surgery (Supplementary Data, Table A and Figure A). Altogether, data confirmed a 24h induced septic shock as previously described (25). Because ROS production was reported to promote senescence (26), we assessed ROS in the thoracic aorta wall. At D7, a 2-fold ROS increase was measured (CLP: 1759±175.2 A.U., *vs.* SHAM: 844.3±49.9 A.U.) the elevation being only 54% after 3 months (Figure 2A). The ROS source was mainly the cell nucleus as confirmed by counterstaining with DAPI. Similar data were found in the abdominal aorta.

Nevertheless, the expression of MMP-9, a matrix metalloproteinase associated with inflammation and senescence (27), was barely detectable in abdominal aorta from both CLP and SHAM animals at D7 by immunostaining but was drastically increased by 5 times in CLP at D90, as demonstrated by confocal microscopy (16.6±2.7 *vs.* 91.1±17.2, $p < 0.05$) (Figure 2B). Furthermore, the MMP-9 expression was mainly detected in the endothelium. While the expression of VCAM-1 and ICAM-1 was similar between CLP and SHAM at D3 in the abdominal or cross aorta (Supplementary data, Figure B.1 and B2), sepsis induced a respective three-fold and two-fold significant up-regulation of VCAM-1 and ICAM-1 in the CLP subset compared to SHAM at D7 ($p < 0.05$) (Figure 2C and 2D), values remaining elevated at D90 at least in the investigated thoracic aorta.

Sepsis induced premature senescence

While no marker of senescence could be detected in the abdominal aortic wall at D3 post peritonitis (Supplementary data, Figure B.3, B.4 and B.5), the expression of p53, the upstream protein of the senescence pathway also associated with apoptosis, and of downstream p21 and p16 was enhanced by respectively 3 folds, 10 folds and 4 folds measured by western blot analysis at D7 ($p < 0.05$; Fig 3A-B-D). Up-regulation of all senescence markers persisted after 3 months (Figure 3A-C-D). The 3-fold elevation in p53, remained stable between D7 and D90, in accordance with the absence of any caspase-3 activation in SHAM or CLP group, thereby excluding apoptosis (Figure 3E). Interestingly, at D90, p21 was only elevated by 5 folds, and the downstream p16 by 3.6 folds, pointing at a senescence-driven pathway, still operating after 3 months, although at a lower range. Moreover, the 3-fold increase in p53 expression was also measured by fluorescence microscopy in the endothelium of the aorta of CLP rats compared to SHAM at D7, a 2.5 enhancement being still observed after 3 months (Figure 3F).

Septic shock is associated to long-term impairment of vascular reactivity

In the thoracic aorta, three months after peritonitis induction, a 50% reduction of the maximal contractile response to PE (Figure 4A) and a 30% reduction in ACH-induced relaxation was observed in CLP group (Figure 4B) with a maximal relaxation at 85% (*vs.* SHAM 55%, $p < 0.05$) (Figure 4B). After indomethacin or L-NA adjunction, the contractile response of CLP aorta was similar compared to untreated SHAM rings (Supplementary data, Figure C.1 and C.2). In the thoracic aorta rings, indomethacin adjunction, a non-selective inhibitor of cyclooxygenases, did not significantly alter the difference between CLP and SHAM Ach-induced relaxation (Supplementary data, Figure D.1). The eNOS inhibitor L-NA abolished the

relaxation to ACh, thereby confirming a major role of nitric oxide (NO) (Supplementary data, Figure D.2).

Altogether, the endothelial dysfunction of the aorta rings 3 months after septic shock was mainly characterized by a blunted NO-component relaxation. In accordance, the aorta protein extracts showed a 40% reduction of eNOS expression occurring in CLP rats as early as D7 and persisting at D90, that was found restricted to the endothelial lining by fluorescence microscopy (Figure 5). No significative difference was found, however, when comparing iNOS expression in both group at D7 and at D90 (Figure 6).

In the main mesenteric artery, three months after peritonitis induction, a 50% reduction of the maximal contractile response to PE (Figure 4C) was observed, however Ach-induced endothelial relaxation remained similar between CLP and SHAM with a maximal relaxation of 80% (Figure 4D). Inhibition of COX by indomethacin and of the endothelium-derived hyperpolarization (EDH)-mediated relaxation in the presence of UCL-1684 plus TRAM-34 (10 μM each) revealed a reduction in Ach-induced relaxation down-to 45% maximal relaxation, that was only evidenced in CLP (Supplementary data, Figure E.1), thereby confirming a blunted NO pathway 90 days after peritonitis. However, adjunction of indomethacin plus L-NA combination indicated a slightly lower (EDH)-component relaxation in CLP as compared to SHAM, although significant was not reached (Supplementary data, Figure E.2). The endothelial dysfunction in mesenteric arteries relaxation was altogether characterized by blunted endothelium-dependent relaxation mainly due to the alteration of the NO pathway and possibly compensated by the prostanoids and EDH (Supplementary data, Figure E.3). Indeed, endothelium-dependent contractile responses was observed in CLP rats compared to SHAM.

A 60% decrease in main mesenteric artery contraction was observed in CLP rats in response to 10-5 M PE and indomethacin adjunction indicated limited involvement of COX-mediated prostanoid pathway (Supplementary data, Figure F.1). In-vitro inhibition of both COX by indomethacin and of the endothelium-derived hyperpolarization (EDH) pathways in the presence of TRAM-34 plus UCL-1684 (10 μM each) indicated a significant dependence on the NO pathway in SHAM rats (50% loss) that was barely significant in CLP rats most likely owing to the downregulation of the eNOS probably reducing availability of NO (Supplementary data, Figure F.2). However, after indomethacin and L-NA adjunction, the contractile response of CLP mesenteric arteries was similar compared to untreated SHAM rings, indicating a dual contribution of prostanoids and NO pathways 3 months after the induction of peritonitis (Supplementary data, Figure F.3). L-NA adjunction alone almost had the same effect (Supplementary data, Figure F.4).

As changes in vascular reactivity are usually associated with wall remodeling, we compared the wall thickness in aorta after 3 months. No differences were found between the SHAM and the CLP group (Supplementary data, Figure G).

Discussion

The present study was designed to assess the long-term impact of sepsis on vascular function. We focused on endothelial senescence as possible mechanism. The main finding was that sepsis induced arterial dysfunction with a time dependent *in situ* acquisition of inflammation and senescence phenotype in both conductance and resistance arteries, therefore pointing at a systemic long-lasting effect.

Our present data confirmed sepsis-induced arterial inflammatory and oxidative stress in the acute phase (28, 29), and highlighted an on-going pro-inflammatory vascular activation until 3 months. Indeed, inflammation and oxidative stress over-expression were maximal at D7 and persisted in the arterial wall at 3 months, confirming their potential impact on sepsis-induced arterial inflammation and atherosclerosis (30-32). Because ROS are known as mediators of both premature and replicative endothelial cell senescence (26, 33, 34), we also investigated SIPS. Furthermore, endothelial senescence is an early indicator of atheroprone vascular sites, suggesting its potential implication in atherogenesis initiation and progression (35). Furthermore, p53 and p21 have been identified as markers of ageing-related senescence in arteries of elderly patients (36). Our present data support the hypothesis that sepsis triggers the premature expression of key transcription factors involved in senescence: p53, p21 and p16 were overexpressed as early as D7 in the abdominal and cross segments of the aorta of septic rats. Overexpression of p53 and downstream p16 was even higher at D90 suggesting amplification over-time. Interestingly, the p53 up-regulation was located in the endothelial layer as demonstrated by confocal microscopy, thereby pointing at endothelial senescence involvement during septic shock. Interestingly, as reported by others (37, 38), apoptosis remained minor.

Because, ageing ECs progressively acquire a dysfunctional phenotype, characterized by pro-oxidant, pro-inflammatory, pro-coagulant alterations, and a drastic loss in nitric oxide

associated to cardiovascular diseases (39), one could potentially advance that septic shock-induced endothelial senescence is a mechanism leading to long-term cardiovascular complications. Indeed, in addition to data confirming that septic shock is associated to systemic arterial dysfunction during the acute phase mainly *via* altered NO pathway (9, 40), we report herein the first long-term persistent vascular dysfunction: our data suggest remote endothelial dysfunction in conductance and resistance arteries that was characterized by long-term blunted endothelium-dependent relaxation and contraction at D90. Interestingly, the selective over-expression of endothelial p53 in rats' aortic rings infected by a p53-expressing adenovirus, reduced endothelium-dependent relaxations and NO formation (41). In line with these observations, our data strongly suggest that p53-induced senescence is pivotal in the initiation and maintenance of endothelial dysfunction. Our data provide new insight on the long-term impairment of NO production and vasoprotection possibly prompted by accelerated senescence after septic shock. Several studies support our observation with a link between sepsis and premature senescence. In a murine endotoxemia model, telomere shortening was observed after 48h in kidney, spleen and blood cells, pointing at a systemic effect (42). In-vitro studies also reported premature senescence after lipopolysaccharides treatment of adipocytes (43), pulmonary epithelial cells (44), microglia cells (45), and dental pulp stem cells (46). In atherosclerosis-prone mice, undeciphered plaque formation occurs along the whole aorta culminating at 5 months after peritonitis indicating accelerated atherogenesis prompted by septic shock (47). Our present data highlight arterial senescence and MMP-9 as potential new mechanistic players, specifically up-regulated in the endothelium after 3 months. This matrix metalloproteinase is involved in pro-inflammatory responses, endothelial dysfunction, atherosclerosis (48) and cardiac senescence by promoting an inflammageing profile (27).

While the Canakinumab Anti-Inflammatory Thrombosis Outcomes Study trial (CANTOS) has proven the feasibility of targeting pro-inflammatory responses to reduce the risk of

cardiovascular events in patients with anti-interleukin-1β therapy, the majority of clinical trials that aimed at controlling the inflammation-mediated vascular responses have failed (49). Interestingly, in critically ill children, inflammation was associated to leukocyte telomere shortening suggesting inflammation-driven senescence (50). Of note, few *in vitro* and *ex vivo* studies describe a link between sustained inflammation and endothelial senescence while endotoxemia was reported to shorten telomeres in rat kidney, spleen and blood tissues with no investigation of endothelial damage (42). Nevertheless, senescent cell displays a pro-inflammatory phenotype termed SASP (senescence-associated secretory phenotype) (51), that may also contribute to accelerated atherothrombosis (52). Therefore, endothelial senescence appears as a promising pharmacological target to limit plaque formation and senotherapy by contributing to the reversal of the senescent phenotype (53-55) should also be considered as a next-generation therapy for septic patients at cardiovascular risk (56, 57). In a trial combining two senolytic drugs, dasatinib, a pan inhibitor of tyrosine kinases, and quercetin, an antioxidant and anti-inflammatory drugs mainly targeting PI3-Kinase and serpins, promising preliminary data were described in patients with cardiovascular risk factors (58, 59). Similarly, in hypercholesterolemic mice chronic treatment by dasatinib and quercetin reduced aortic calcification and consecutive loss of cardiovascular function (60). In a myocardial infarction model of aged mice, administration of ABT263 another senolytic drug improved myocardial remodeling, diastolic function, and overall survival (61).

Study limitations: Endothelial senescence is probably not the only mechanism by which sepsis promotes atheroma. Although standardized, peritonitis-induced sepsis probably leads to several pathogens load from one animal to another, resulting in a complex host response. Thus, the number of molecular and cellular pathways that could potentially underlie the effects of sepsis is huge and will require exploring other paths.

We report a new model of long-term septic shock-induce vascular dysfunction that was associated with persisting endothelium senescence and pro-inflammatory responses. Our data highlight the crucial needs for a long-term evaluation in sepsis since pro-inflammatory and pro-senescent vascular effectors, that are barely detectable, may drastically accumulate over time and alter the endothelial response.

Conclusion

The present findings indicate that sepsis accelerates endothelial senescence and induces persistent vascular dysfunction. Timely acquisition of a senescence-induced endothelial and vascular dysfunction may partly explain atherosclerosis in sepsis survivors. Targeting pro-senescent endothelial cells with senolytics in sepsis may be of interest to delay endothelial senescence and improve vascular health and long-term outcome of sepsis.

References

1. Singer M, Deutschman CS, Seymour CW, Shankar-Hari M, Annane D, Bauer M, et al. The Third International Consensus Definitions for Sepsis and Septic Shock (Sepsis-3). JAMA. 2016;315(8):801-10.
2. Reinhart K, Daniels R, Kissoon N, Machado FR, Schachter RD, Finfer S. Recognizing Sepsis as a Global Health Priority - A WHO Resolution. N Engl J Med. 2017;377(5):414-7.
3. Rudd KE, Johnson SC, Agesa KM, Shackelford KA, Tsoi D, Kievlan DR, et al. Global, regional, and national sepsis incidence and mortality, 1990-2017: analysis for the Global Burden of Disease Study. Lancet. 2020;395(10219):200-11.
4. Vincent JL, Rello J, Marshall J, Silva E, Anzueto A, Martin CD, et al. International study of the prevalence and outcomes of infection in intensive care units. JAMA. 2009;302(21):2323-9.
5. Fleischmann C, Scherag A, Adhikari NK, Hartog CS, Tsaganos T, Schlattmann P, et al. Assessment of Global Incidence and Mortality of Hospital-treated Sepsis. Current Estimates and Limitations. Am J Respir Crit Care Med. 2016;193(3):259-72.
6. Shankar-Hari M, Rubenfeld GD. Understanding Long-Term Outcomes Following Sepsis: Implications and Challenges. Curr Infect Dis Rep. 2016;18(11):37.
7. Rizzo AN, Belvitch P, Demeritte R, Garcia JGN, Letsiou E, Dudek SM. Arg mediates LPS-induced disruption of the pulmonary endothelial barrier. Vascul Pharmacol. 2020;128-129:106677.
8. Dolmatova EV, Wang K, Mandavilli R, Griendling KK. The effects of sepsis on endothelium and clinical implications. Cardiovasc Res. 2021;117(1):60-73.
9. Boisrame-Helms J, Kremer H, Schini-Kerth V, Meziani F. Endothelial dysfunction in sepsis. Curr Vasc Pharmacol. 2013;11(2):150-60.
10. Park KH, Park WJ. Endothelial Dysfunction: Clinical Implications in Cardiovascular Disease and Therapeutic Approaches. J Korean Med Sci. 2015;30(9):1213-25.
11. Prescott HC, Osterholzer JJ, Langa KM, Angus DC, Iwashyna TJ. Late mortality after sepsis: propensity matched cohort study. BMJ. 2016;353:i2375.
12. Wu MH, Tsou PY, Wang YH, Lee MG, Chao CCT, Lee WC, et al. Impact of post-sepsis cardiovascular complications on mortality in sepsis survivors: a population-based study. Crit Care. 2019;23(1):293.
13. Mankowski RT, Yende S, Angus DC. Long-term impact of sepsis on cardiovascular health. Intensive Care Med. 2019;45(1):78-81.
14. Toussaint O, Medrano EE, von Zglinicki T. Cellular and molecular mechanisms of stress-induced premature senescence (SIPS) of human diploid fibroblasts and melanocytes. Exp Gerontol. 2000;35(8):927-45.
15. Rufini A, Tucci P, Celardo I, Melino G. Senescence and aging: the critical roles of p53. Oncogene. 2013;32(43):5129-43.
16. Herranz N, Gil J. Mechanisms and functions of cellular senescence. J Clin Invest. 2018;128(4):1238-46.
17. Jia G, Aroor AR, Jia C, Sowers JR. Endothelial cell senescence in aging-related vascular dysfunction. Biochim Biophys Acta Mol Basis Dis. 2019;1865(7):1802-9.
18. Katsuumi G, Shimizu I, Yoshida Y, Minamino T. Vascular Senescence in Cardiovascular and Metabolic Diseases. Front Cardiovasc Med. 2018;5:18.
19. Vasile E, Tomita Y, Brown LF, Kocher O, Dvorak HF. Differential expression of thymosin beta-10 by early passage and senescent vascular endothelium is modulated by

VPF/VEGF: evidence for senescent endothelial cells in vivo at sites of atherosclerosis. FASEB J. 2001;15(2):458-66.
20. Buras JA, Holzmann B, Sitkovsky M. Animal models of sepsis: setting the stage. Nat Rev Drug Discov. 2005;4(10):854-65.
21. Rittirsch D, Huber-Lang MS, Flierl MA, Ward PA. Immunodesign of experimental sepsis by cecal ligation and puncture. Nat Protoc. 2009;4(1):31-6.
22. Abraldes JG, Iwakiri Y, Loureiro-Silva M, Haq O, Sessa WC, Groszmann RJ. Mild increases in portal pressure upregulate vascular endothelial growth factor and endothelial nitric oxide synthase in the intestinal microcirculatory bed, leading to a hyperdynamic state. Am J Physiol Gastrointest Liver Physiol. 2006;290(5):G980-7.
23. Idris Khodja N, Chataigneau T, Auger C, Schini-Kerth VB. Grape-derived polyphenols improve aging-related endothelial dysfunction in rat mesenteric artery: role of oxidative stress and the angiotensin system. PLoS One. 2012;7(2):e32039.
24. Zhai X, Yang Z, Zheng G, Yu T, Wang P, Liu X, et al. Lactate as a Potential Biomarker of Sepsis in a Rat Cecal Ligation and Puncture Model. Mediators Inflamm. 2018;2018:8352727.
25. Boisrame-Helms J, Delabranche X, Degirmenci SE, Zobairi F, Berger A, Meyer G, et al. Pharmacological modulation of procoagulant microparticles improves haemodynamic dysfunction during septic shock in rats. Thromb Haemost. 2014;111(1):154-64.
26. Abbas M, Jesel L, Auger C, Amoura L, Messas N, Manin G, et al. Endothelial Microparticles From Acute Coronary Syndrome Patients Induce Premature Coronary Artery Endothelial Cell Aging and Thrombogenicity: Role of the Ang II/AT1 Receptor/NADPH Oxidase-Mediated Activation of MAPKs and PI3-Kinase Pathways. Circulation. 2017;135(3):280-96.
27. Ma Y, Chiao YA, Clark R, Flynn ER, Yabluchanskiy A, Ghasemi O, et al. Deriving a cardiac ageing signature to reveal MMP-9-dependent inflammatory signalling in senescence. Cardiovasc Res. 2015;106(3):421-31.
28. Kremer H, Baron-Menguy C, Tesse A, Gallois Y, Mercat A, Henrion D, et al. Human serum albumin improves endothelial dysfunction and survival during experimental endotoxemia: concentration-dependent properties. Crit Care Med. 2011;39(6):1414-22.
29. Joffre J, Hellman J, Ince C, Ait-Oufella H. Endothelial Responses in Sepsis. Am J Respir Crit Care Med. 2020;202(3):361-70.
30. Back M, Yurdagul A, Jr., Tabas I, Oorni K, Kovanen PT. Inflammation and its resolution in atherosclerosis: mediators and therapeutic opportunities. Nat Rev Cardiol. 2019;16(7):389-406.
31. Wolf D, Ley K. Immunity and Inflammation in Atherosclerosis. Circ Res. 2019;124(2):315-27.
32. Gager GM, Biesinger B, Hofer F, Winter MP, Hengstenberg C, Jilma B, et al. Interleukin-6 level is a powerful predictor of long-term cardiovascular mortality in patients with acute coronary syndrome. Vascul Pharmacol. 2020;135:106806.
33. Burger D, Kwart DG, Montezano AC, Read NC, Kennedy CR, Thompson CS, et al. Microparticles induce cell cycle arrest through redox-sensitive processes in endothelial cells: implications in vascular senescence. J Am Heart Assoc. 2012;1(3):e001842.
34. Khemais-Benkhiat S, Idris-Khodja N, Ribeiro TP, Silva GC, Abbas M, Kheloufi M, et al. The Redox-sensitive Induction of the Local Angiotensin System Promotes Both Premature and Replicative Endothelial Senescence: Preventive Effect of a Standardized Crataegus Extract. J Gerontol A Biol Sci Med Sci. 2016;71(12):1581-90.

35. Warboys CM, de Luca A, Amini N, Luong L, Duckles H, Hsiao S, et al. Disturbed flow promotes endothelial senescence via a p53-dependent pathway. Arterioscler Thromb Vasc Biol. 2014;34(5):985-95.
36. Morgan RG, Ives SJ, Lesniewski LA, Cawthon RM, Andtbacka RH, Noyes RD, et al. Age-related telomere uncapping is associated with cellular senescence and inflammation independent of telomere shortening in human arteries. Am J Physiol Heart Circ Physiol. 2013;305(2):H251-8.
37. Hotchkiss RS, Tinsley KW, Swanson PE, Karl IE. Endothelial cell apoptosis in sepsis. Crit Care Med. 2002;30(5 Suppl):S225-8.
38. Childs BG, Baker DJ, Kirkland JL, Campisi J, van Deursen JM. Senescence and apoptosis: dueling or complementary cell fates? EMBO Rep. 2014;15(11):1139-53.
39. Machado-Oliveira G, Ramos C, Marques ARA, Vieira OV. Cell Senescence, Multiple Organelle Dysfunction and Atherosclerosis. Cells. 2020;9(10).
40. Ince C, Mayeux PR, Nguyen T, Gomez H, Kellum JA, Ospina-Tascon GA, et al. The Endothelium in Sepsis. Shock. 2016;45(3):259-70.
41. Kumar A, Kim CS, Hoffman TA, Naqvi A, Dericco J, Jung SB, et al. p53 impairs endothelial function by transcriptionally repressing Kruppel-Like Factor 2. Arterioscler Thromb Vasc Biol. 2011;31(1):133-41.
42. Oliveira NM, Rios ECS, de Lima TM, Victorino VJ, Barbeiro H, Pinheiro da Silva F, et al. Sepsis induces telomere shortening: a potential mechanism responsible for delayed pathophysiological events in sepsis survivors? Mol Med. 2017;22:886-91.
43. Zhao M, Chen X. Effect of lipopolysaccharides on adipogenic potential and premature senescence of adipocyte progenitors. Am J Physiol Endocrinol Metab. 2015;309(4):E334-44.
44. Kim CO, Huh AJ, Han SH, Kim JM. Analysis of cellular senescence induced by lipopolysaccharide in pulmonary alveolar epithelial cells. Arch Gerontol Geriatr. 2012;54(2):e35-41.
45. Yu HM, Zhao YM, Luo XG, Feng Y, Ren Y, Shang H, et al. Repeated lipopolysaccharide stimulation induces cellular senescence in BV2 cells. Neuroimmunomodulation. 2012;19(2):131-6.
46. Feng X, Feng G, Xing J, Shen B, Tan W, Huang D, et al. Repeated lipopolysaccharide stimulation promotes cellular senescence in human dental pulp stem cells (DPSCs). Cell Tissue Res. 2014;356(2):369-80.
47. Kaynar AM, Yende S, Zhu L, Frederick DR, Chambers R, Burton CL, et al. Effects of intra-abdominal sepsis on atherosclerosis in mice. Crit Care. 2014;18(5):469.
48. Florence JM, Krupa A, Booshehri LM, Allen TC, Kurdowska AK. Metalloproteinase-9 contributes to endothelial dysfunction in atherosclerosis via protease activated receptor-1. PLoS One. 2017;12(2):e0171427.
49. Ridker PM, Everett BM, Thuren T, MacFadyen JG, Chang WH, Ballantyne C, et al. Antiinflammatory Therapy with Canakinumab for Atherosclerotic Disease. N Engl J Med. 2017;377(12):1119-31.
50. Verstraete S, Vanhorebeek I, van Puffelen E, Derese I, Ingels C, Verbruggen SC, et al. Leukocyte telomere length in paediatric critical illness: effect of early parenteral nutrition. Crit Care. 2018;22(1):38.
51. Childs BG, Gluscevic M, Baker DJ, Laberge RM, Marquess D, Dananberg J, et al. Senescent cells: an emerging target for diseases of ageing. Nat Rev Drug Discov. 2017;16(10):718-35.

52. Ruparelia N, Choudhury R. Inflammation and atherosclerosis: what is on the horizon? Heart. 2020;106(1):80-5.
53. Baker DJ, Wijshake T, Tchkonia T, LeBrasseur NK, Childs BG, van de Sluis B, et al. Clearance of p16Ink4a-positive senescent cells delays ageing-associated disorders. Nature. 2011;479(7372):232-6.
54. Xu M, Pirtskhalava T, Farr JN, Weigand BM, Palmer AK, Weivoda MM, et al. Senolytics improve physical function and increase lifespan in old age. Nat Med. 2018;24(8):1246-56.
55. Misuth S, Uhrinova M, Klimas J, Vavrincova-Yaghi D, Vavrinec P. Vildagliptin improves vascular smooth muscle relaxation and decreases cellular senescence in the aorta of doxorubicin-treated rats. Vascul Pharmacol. 2021;138:106855.
56. Childs BG, Baker DJ, Wijshake T, Conover CA, Campisi J, van Deursen JM. Senescent intimal foam cells are deleterious at all stages of atherosclerosis. Science. 2016;354(6311):472-7.
57. Dookun E, Passos JF, Arthur HM, Richardson GD. Therapeutic Potential of Senolytics in Cardiovascular Disease. Cardiovasc Drugs Ther. 2020.
58. Hickson LJ, Langhi Prata LGP, Bobart SA, Evans TK, Giorgadze N, Hashmi SK, et al. Senolytics decrease senescent cells in humans: Preliminary report from a clinical trial of Dasatinib plus Quercetin in individuals with diabetic kidney disease. EBioMedicine. 2019;47:446-56.
59. Chang J, Wang Y, Shao L, Laberge RM, Demaria M, Campisi J, et al. Clearance of senescent cells by ABT263 rejuvenates aged hematopoietic stem cells in mice. Nat Med. 2016;22(1):78-83.
60. Roos CM, Zhang B, Palmer AK, Ogrodnik MB, Pirtskhalava T, Thalji NM, et al. Chronic senolytic treatment alleviates established vasomotor dysfunction in aged or atherosclerotic mice. Aging Cell. 2016;15(5):973-7.
61. Walaszczyk A, Dookun E, Redgrave R, Tual-Chalot S, Victorelli S, Spyridopoulos I, et al. Pharmacological clearance of senescent cells improves survival and recovery in aged mice following acute myocardial infarction. Aging Cell. 2019;18(3):e12945.

Figure legends

Figure 1:
Time scale of the experimental protocol**.**

Figure 2:
2A: Sepsis induces a persistent vascular up-regulation of ROS in aorta rings at D7 and D90. ROS were labelled in aorta rings by DHE probing (red) at D7 ($p = 0.02$) and D90 ($p = 0.03$). Sections were counterstained with DAPI to identify the nucleus. Endothelium is facing the right part of each quadrant. **2B:** Sepsis induces a persistent endothelial up-regulation of MMP-9 in abdominal aorta rings at D7 ($p = 0.22$) and D90 ($p = 0.01$). Endothelium is facing the right part of each quadrant. **2C:** Sepsis induces a persistent up-regulation of ICAM-1 expression in aorta extracts at D7 ($p = 0.04$) and D90 ($p = 0.06$). **2D:** Sepsis induces a persistent up-regulation of VCAM-1 expression in aorta extracts at D7 ($p = 0.19$) and D90 ($p = 0.01$). Data are expressed as mean and standard deviation (SD). D7 : SHAM n = 6 ; CLP n = 7 and D90 : SHAM n = 11 ; CLP n = 8. Unpaired Student's t-test was applied. * $p < 0.05$.

Figure 3:
3A: Sepsis induces a persistent vascular up-regulation of p53 in aorta extracts at D7 ($p = 0.01$) and D90 ($p = 0.04$). **3B and 3C:** Sepsis induces a persistent vascular up-regulation of p21 in aorta extracts at D7 (3B) ($p = 0.03$) and D90 (3C) ($p = 0.04$). **3D:** Sepsis induces a persistent vascular up-regulation of p16 in aorta extracts at D7 ($p = 0.01$) and D90 ($p = 0.004$). **3E:** Caspase 3 expression in aorta extracts was measured at D7 ($p = 0.09$) and D90 ($p = 0.1$). **3F:** Sepsis induces a persistent endothelial up-regulation of p53 in abdominal aorta rings at D7 ($p = 0.02$) and D90 ($p = 0.001$). Data are expressed as mean and standard deviation (SD). D7: SHAM n = 6 ; CLP n = 7 and D90: SHAM n = 11 ; CLP n = 8. Unpaired Student's t-test was applied. * $p < 0.05$. Endothelium is facing the right part of each quadrant.

Figure 4:
Effect of sepsis on the endothelium-dependent contractile response to phenylephrine **(4A)** ($p < 0.0001$) and the endothelium-dependent relaxation to acetylcholine **(4B)** on aorta rings at D90 ($p = 0.01$). Effect of sepsis on the endothelium-dependent contractile response to phenylephrine **(4C)** ($p = 0.0001$) and the endothelium-dependent relaxation to acetylcholine **(4D)** on main mesenteric artery rings at D90 ($p > 0,9$). Values are shown as mean and standard deviation (SD). SHAM n = 5 ; CLP n = 7. Two-way ANOVA test was applied. * $p < 0.05$.

Figure 5:
Sepsis induces a persistent endothelial down-regulation of eNOS in aorta rings at D7 ($p = 0.04$) and at D90 ($p = 0.006$). Endothelium is facing the right part of each quadrant. Data are expressed as mean and standard deviation (SD). SHAM n = 6 ; CLP n = 6. Unpaired Student's t-test was applied. * $p < 0.05$.

Figure 6:
Sepsis induces a non-significative up-regulation of iNOS in aorta rings at D7 ($p = 0.1$) and at D90 ($p = 0.9$). Endothelium is facing the right part of each quadrant. Data are expressed as

mean and standard deviation (SD). SHAM n = 6 ; CLP n = 6. Unpaired Student's t-test was applied. * $p < 0.05$.

Appendices

Supplementary data

Table A:
Blood lactate concentration in SHAM and CLP rats was measured after 24H. Blood pressure in SHAM and CLP was measured 24h after surgery. SHAM n = 8 ; CLP n = 15. Unpaired Student's t-test was applied. Data are expressed as mean and standard deviation (SD).

Figure A:
Kaplan–Meier survival curves for SHAM and CLP rats after seven days. SHAM n = 6 ; CLP n = 10.

Figure B:
No differences were observed regarding ICAM-1 **(B.1)** ($p = 0.8$) and VCAM-1 **(B.2)** ($p = 0.8$) at D3. No differences were observed regarding p53 **(B.3)** ($p > 0.9$)**,** p21 **(B.4)** ($p = 0.9$) and p16 **(B.5)** ($p = 0.2$) at D3. SHAM n = 6 ; CLP n = 7. Unpaired Student's t-test was applied. Data are expressed as mean and standard deviation (SD).

Figure C:
No differences were observed regarding Aorta contraction either with indomethacin (C.1) or L-NA (C.2).
SHAM n = 5 ; CLP n = 7. Two-way ANOVA test was applied.

Figure D:
D.1: NO component of relaxation assessed in the presence of indomethacin (10 μM) on aorta rings at D90 ($p = 0.02$). **D.2**: PROSTANOIDS component of relaxation assessed in the presence of Nω-nitro-l-arginine (L-NA, 300 μM) on aorta rings at D90 ($p = 0.8$). Data are expressed as mean and standard deviation (SD). SHAM n = 5 ; CLP n = 7. Two-way ANOVA test was applied. * $p < 0.05$.

Figure E:
E.1: NO component of relaxation assessed in the presence of indomethacin (10 μM) plus UCL-1684 plus TRAM-34 (1 μM each) on main mesenteric artery rings at D90 ($p = 0.02$). **E.2:** EDH component of relaxation assessed in the presence of indomethacin (10 μM) and L-NA (300 μM) on main mesenteric artery rings at D90 ($p = 0.16$). **E.3:** NO and EDH component of relaxation assessed in the presence of indomethacin (10 μM) on main mesenteric artery rings at D90 ($p = 0.01$). Data are expressed as mean and standard deviation (SD). Two-way ANOVA test was applied. SHAM n = 5 ; CLP n = 7. * $p < 0.05$.

Figure F:
F.1: NO and EDHF component of contraction assessed in the presence of indomethacin (10 μM) on mesenteric arteries ($p = 0.004$). **F.2:** NO component of contraction assessed in the presence of indomethacin (10 μM) plus UCL-1684 plus TRAM-34 (1 μM each) on main mesenteric artery at D90 ($p > 0.9$). **F.3:** EDH component of contraction assessed in the presence

of indomethacin (10 μM) and L-NA (300 μM) on main mesenteric artery at D90 ($p > 0.9$). Data are expressed as mean and standard deviation (SD). SHAM n = 5 ; CLP n = 7. Two-way ANOVA test was applied. * $p < 0.05$.

Figure G:
No differences were observed regarding wall thickness between SHAM an CLP aorta at D7 and at D90. Data are expressed as mean and standard deviation (SD). Unpaired Student's t-test was applied. SHAM n = 6 ; CLP n = 6.

D0 D1 D3 D7 D90

CLP

SHAM

WB

- WB
- Immunostaining

- Western Blot (WB)
- Blood lactate level assessment
- Arterial pressure monitoring

- WB
- Immunostaining
- Vascular reactivity assessment

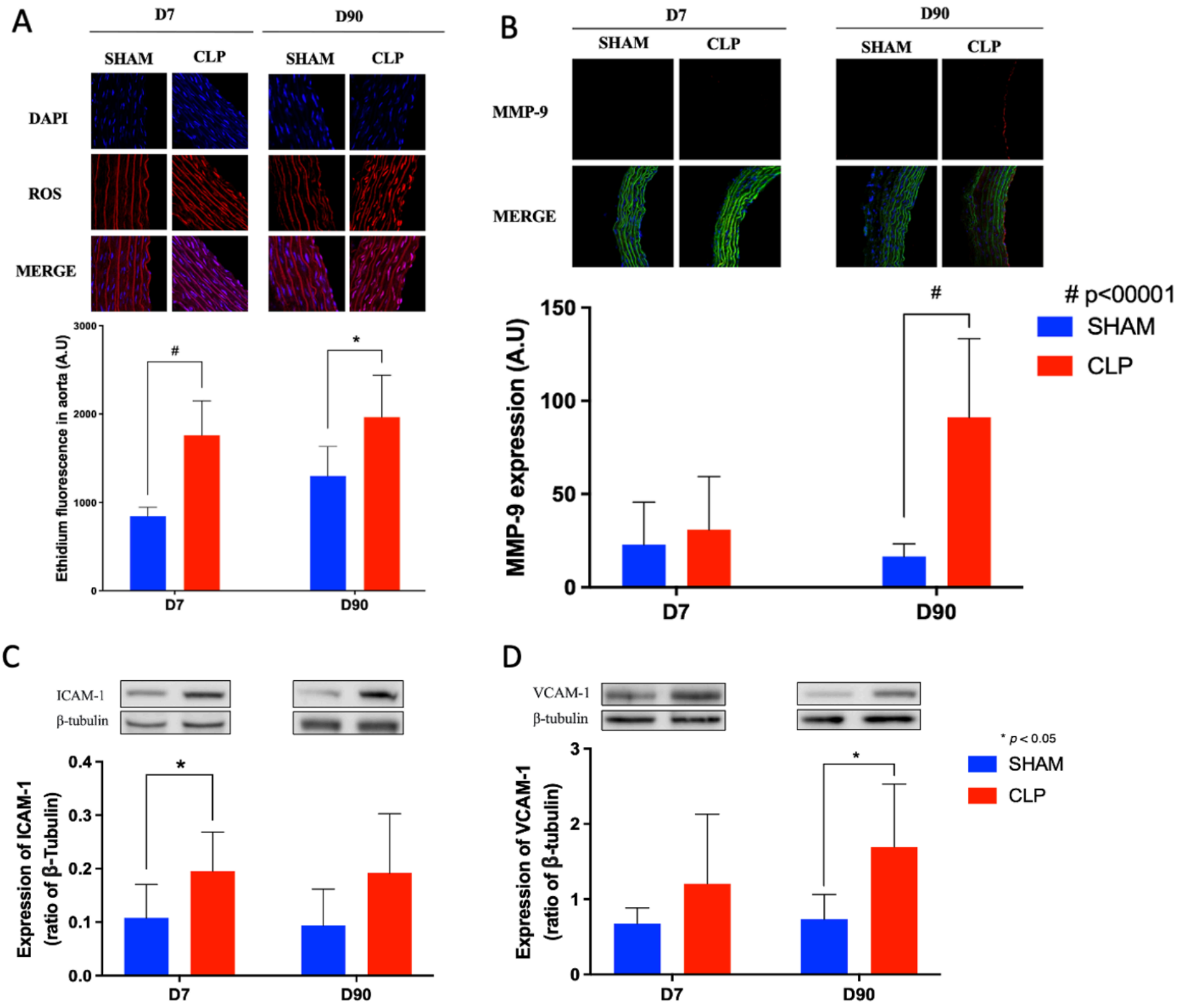
A
D7
D90
SHAM
CLP
SHAM
CLP
DAPI
ROS
MERGE
Ethidium fluorescence in aorta (A.U)
3000
2000
1000
0
#
*
D7
D90
B
D7
D90
SHAM
CLP
SHAM
CLP
MMP-9
MERGE
MMP-9 expression (A.U)
150
100
50
0
#
p<00001
SHAM
CLP
D7
D90
C
ICAM-1
β-tubulin
Expression of ICAM-1 (ratio of β-Tubulin)
0.4
0.3
0.2
0.1
0.0
*
D7
D90
D
VCAM-1
β-tubulin
Expression of VCAM-1 (ratio of β-tubulin)
3
2
1
0
*
* p < 0.05
SHAM
CLP
D7
D90

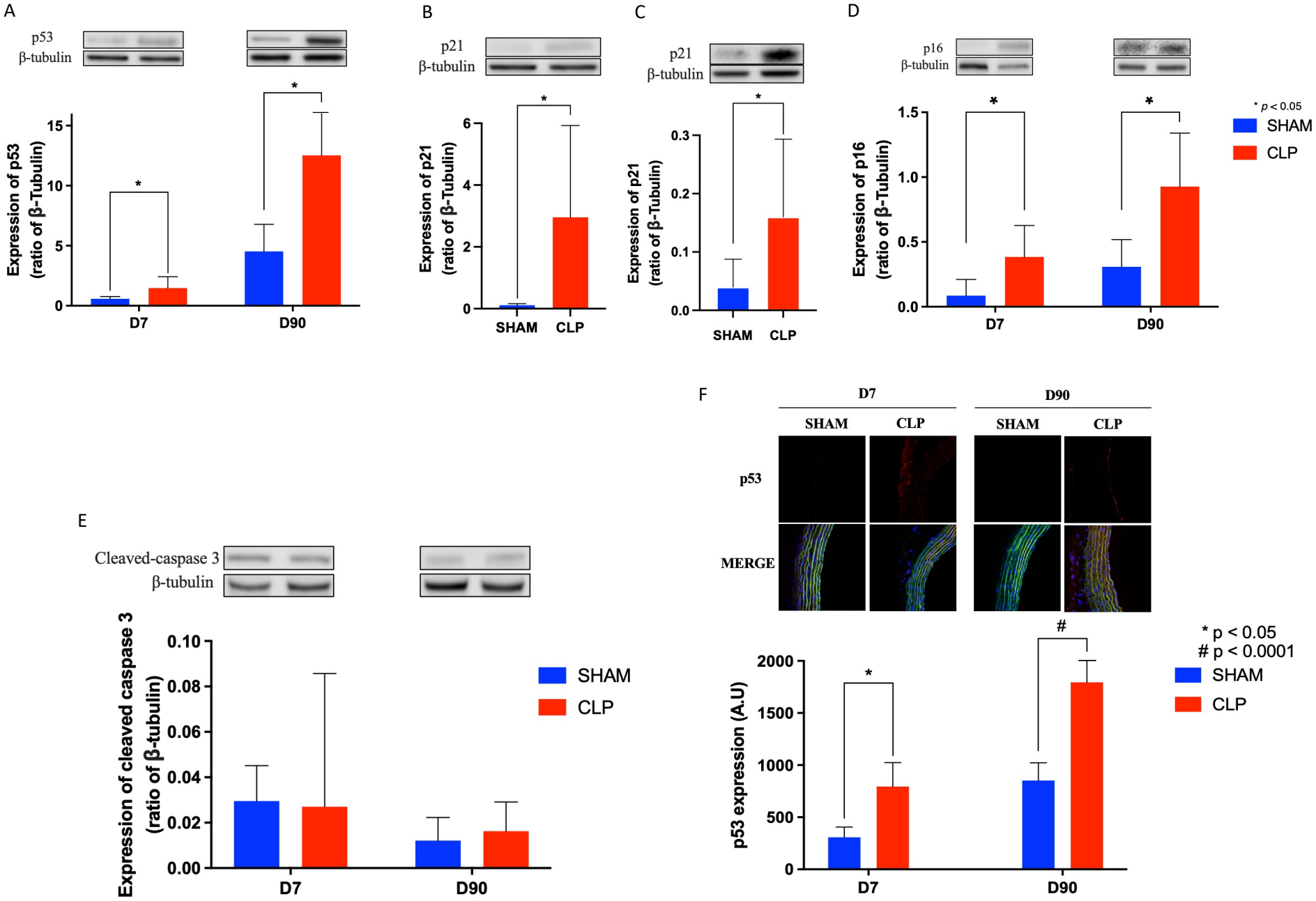
A
p53
β-tubulin
Expression of p53 (ratio of β-Tubulin)
D7
D90
B
p21
β-tubulin
Expression of p21 (ratio of β-Tubulin)
SHAM
CLP
C
p21
β-tubulin
Expression of p21 (ratio of β-Tubulin)
SHAM
CLP
D
p16
β-tubulin
Expression of p16 (ratio of β-Tubulin)
D7
D90
* p < 0.05
SHAM
CLP
E
Cleaved-caspase 3
β-tubulin
Expression of cleaved caspase 3 (ratio of β-tubulin)
D7
D90
SHAM
CLP
F
D7
D90
SHAM
CLP
SHAM
CLP
p53
MERGE
p53 expression (A.U)
D7
D90
* p < 0.05
# p < 0.0001
SHAM
CLP

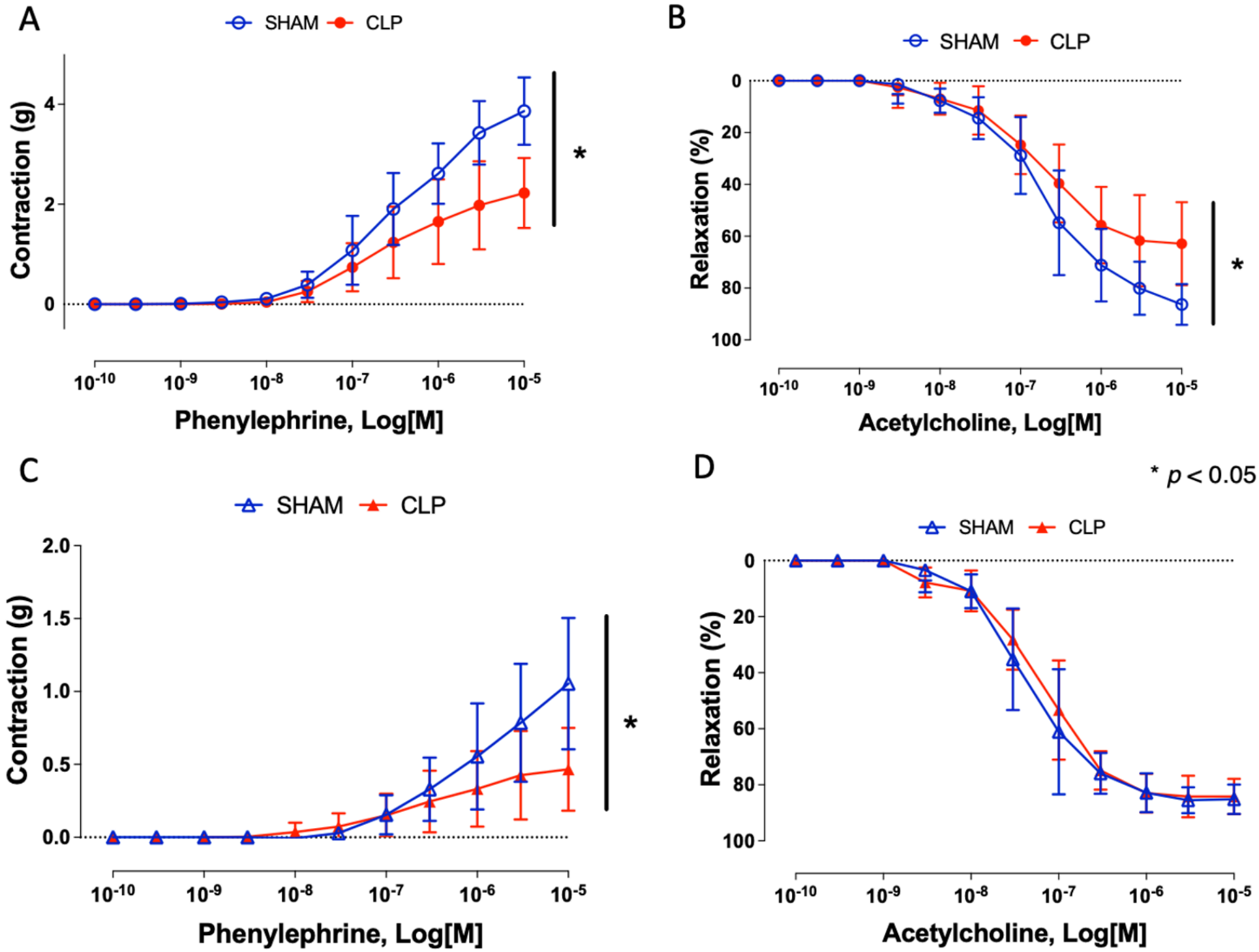
A
SHAM
CLP
Contraction (g)
0
2
4
*
10-10
10-9
10-8
10-7
10-6
10-5
Phenylephrine, Log[M]
B
SHAM
CLP
Relaxation (%)
0
20
40
60
80
100
*
10-10
10-9
10-8
10-7
10-6
10-5
Acetylcholine, Log[M]
C
SHAM
CLP
Contraction (g)
0.0
0.5
1.0
1.5
2.0
*
10-10
10-9
10-8
10-7
10-6
10-5
Phenylephrine, Log[M]
D
* p < 0.05
SHAM
CLP
Relaxation (%)
0
20
40
60
80
100
10-10
10-9
10-8
10-7
10-6
10-5
Acetylcholine, Log[M]

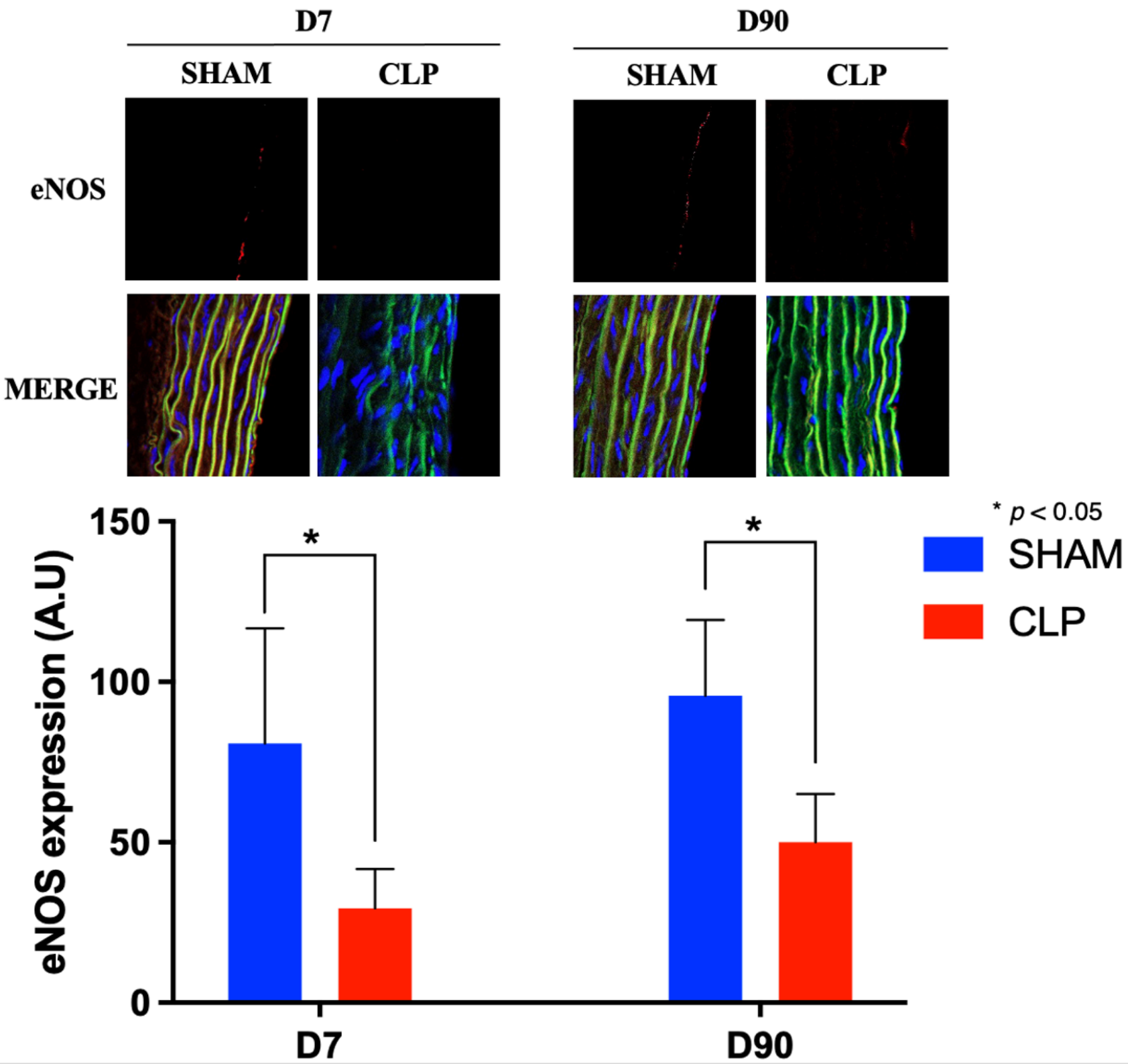
D7
D90
SHAM
CLP
SHAM
CLP
eNOS
MERGE
150
100
50
0
eNOS expression (A.U)
*
*
D7
D90
* p < 0.05
SHAM
CLP

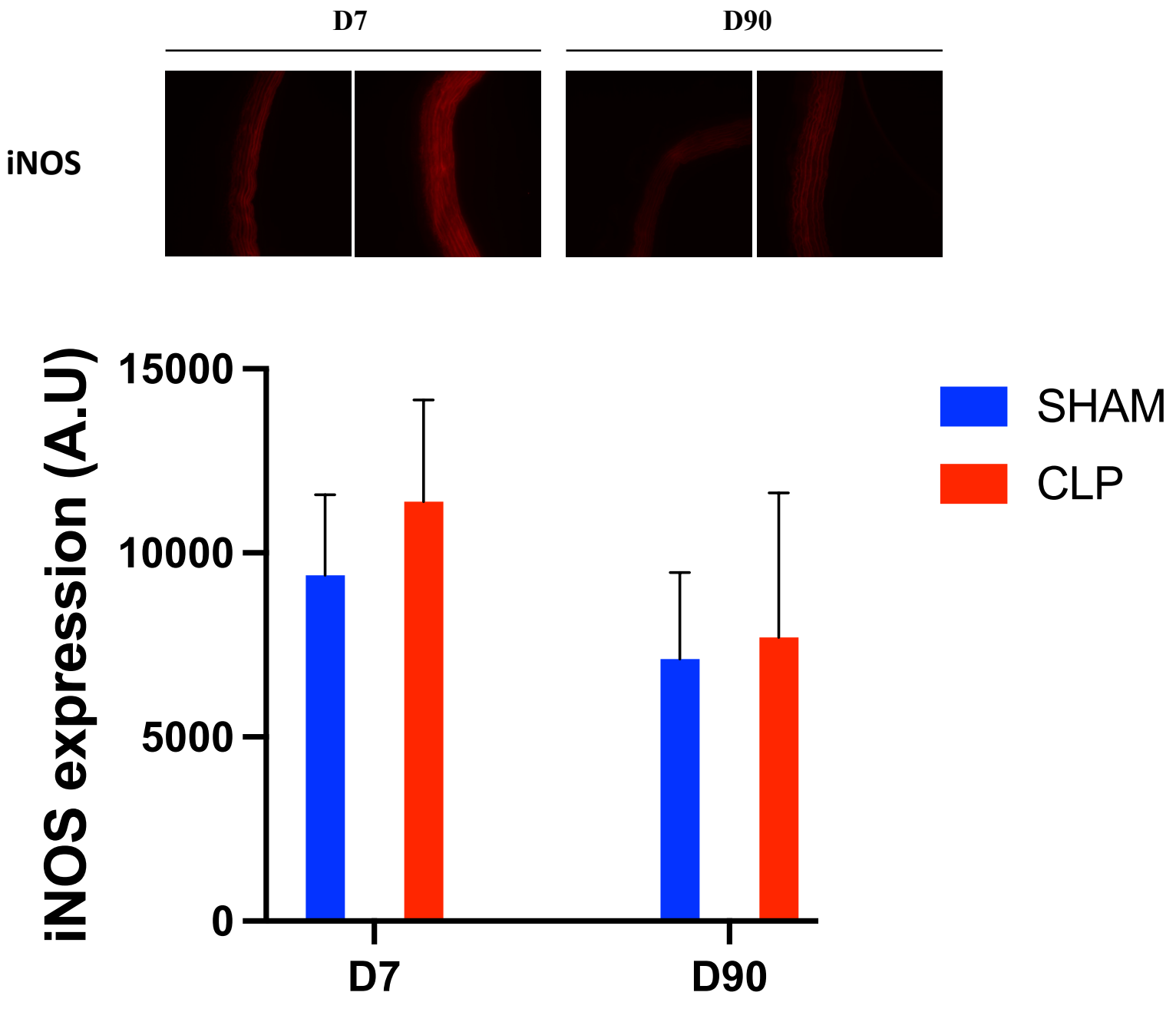
D7
D90
iNOS
iNOS expression (A.U)
15000
10000
5000
0
D7
D90
SHAM
CLP